Biochemical and Biophysical Research Communications 459 (2015) 10–17

Contents lists available at ScienceDirect

Biochemical and Biophysical Research Communications

journal homepage: www.elsevier.com/locate/ybbrc

Inhibition of H3K9 methyltransferase G9a induces autophagy and apoptosis in oral squamous cell carcinoma

Aishu Ren [a, b], Yu Qiu [a, b], Hongjuan Cui [c], Gang Fu [a, b, *]

[a] Chongqing Key Laboratory for Oral Diseases and Biomedical Sciences, Chongqing Medical University, Chongqing, 401147, PR China
[b] Affiliated Hospital of Stomatology, Chongqing Medical University, Chongqing, 401147, PR China
[c] State Key Laboratory of Silkworm Genome Biology, Southwest University, Chongqing, 400716, PR China

ARTICLE INFO

Article history:
Received 12 January 2015
Available online 26 January 2015

Keywords:
G9a
Oral squamous cell carcinoma (OSCC)
Autophagy
Apoptosis

ABSTRACT

Objective: To explore whether inhibition of H3K9 Methyltransferase G9a could exert an antitumoral effect in oral squamous cell carcinoma (OSCC).
Materials and methods: First we checked G9a expression in two OSCC cell lines Tca8113 and KB. Next we used a special G9a inhibitor BIX01294 (BIX) to explore the effect of inhibition of G9a on OSCC in vitro. Cell growth was tested by typlan blue staining, MTT assay and Brdu immunofluorescence staining. Cell autophagy was examined by monodansylcadaverine (MDC) staining, LC3-II immunofluorescence staining and LC3-II western blot assay. Cell apoptosis was checked by FITC Annexin-V and PI labeling, tunnel staining and caspase 3 western blot assay. Finally, the effect of inhibition of G9a on clonogenesis and tumorigenesis capacity of OSCC was analyzed by soft agar growth and xenograft model.
Results: Here we showed that G9a was expressed in both Tca8113 and KB cells. Inhibition of G9a using BIX significantly reduced cell growth and proliferation in Tca8113 and KB. Inhibition of G9a induced cell autophagy with conversion of LC3-I to LC3-II and cell apoptosis with the expression of cleaved caspase 3. We also found that inhibition of G9a reduced colony formation in soft agar and repressed tumor growth in mouse xenograph model.
Conclusion: Our results suggested that G9a might be a potential epigenetic target for OSCC treatment.

1. Introduction

Oral squamous cell carcinoma (OSCC) represents more than 80% of all forms of head and neck cancer, and during the past decade its incidence has increased by 50% [1–3]. Although there have been some progress in the treatment of OSCC, the five-year survival rate of these patients is only 50% [4], which is still one of the lowest among all major human cancers [5], and has not improved in the past three decades [4]. In addition, a high percentage of patients have a poor response to therapy and high recurrence rates [6]. Therefore it is particularly important to identify some new target point for OSCC treatment.

Epigenetic mechanism plays an important role during carcinogenesis. Epigenetics defines all meiotically and mitotically heritable changes in gene expression that are not coded in the DNA sequence itself [7]. Histone methylation is one of the main epigenetic mechanism and linked to the silencing of a number of critical tumor suppressor genes in tumorigenesis [8,9]. G9a, also known as EHMT2, is a H3K9 methyltransferase that has a primary role in catalyzing monomethylation and dimethylation of H3K9 (H3K9me1 and H3K9me2) in euchromatin [10–13]. Elevated levels of G9a expression have been observed in many types of human cancers, and are involved in proliferation and metastasis of various cancer cells [14–16].

In this study, we investigated the role of G9a in OSCC growth using a special G9a inhibitor BIX01294. The result showed that inhibition of G9a could reduce growth and proliferation, and induce autophagy and apoptosis in OSCC. We also found that inhibition of G9a reduced colony formation in soft agar and repressed tumor growth in a xenograft model. Our results provided experimental support for the important role of G9a in regulation growth and death in OSCC.

* Corresponding author. Affiliated Hospital of Stomatology, Chongqing Medical University, # 426, North Songshi Road, Chongqing, 401147, PR China.
E-mail address: fg.ras@hotmail.com (G. Fu).

http://dx.doi.org/10.1016/j.bbrc.2015.01.068
0006-291X/

2. Materials and methods

2.1. Cell culture

Human OSCC cell lines Tca8113 and KB were purchased from Shanghai cell bank, Chinese Academy of Science. Both cells were grown in RPMI 1640 supplemented with 10% fetal bovine serum (FBS) and 1% antibiotics penicillin and streptomycin (P/S). The growth media, FBS and antibiotics were purchased from Gibco. The cells were cultured at 37 °C in a 5% CO_2 humidified incubators.

2.2. Cell growth assay

G9a inhibitor BIX01294 (BIX, Sigma) was dissolved in sterile water. Tca8113 and KB cells were seed in 6-well plate at 20,000 cell per well for overnight. Then the cells were treated with BIX at 0.5 μM, 1 μM, 5 μM, 10 μM or 20 μM for 48 h. Micrographs of cell morphology were taken by an inverted microscopy (Olympus). Cells were collected and calculated by Trypan Blue assay.

Cell viability was further determined using MTT assay. Cells were seed in 96-well plate at 1000 cell per well for overnight. Then the cells were treated with 5 μM BIX. After indicated time period, 20 μl MTT (5 mg/ml, Sigma) was added to each well and incubated at 37 °C for 4 h, and then removed the supernatant. 200 μl DMSO was used to each well to dissolve the cell pellets. After shaking for 15 min, the absorbance was measured at a wavelength of 560 nm.

2.3. Brdu staining

Cells were grown on coverslips and treated with 5 μM BIX for 48 h. The BrdU (Sigma) stock solution at 10 mg/ml was diluted 1000× in the culture medium and incubated for 30 min. Cells were washed with PBS, fixed in 4% paraformaldehyde (PFA) for 20 min, and permeabilized with 2 M HCl for 15 min and 1% Triton X-100 for 15 min. The cells were blocked with 10% goat serum for 1 h, incubated with a primary rat antibody against BrdU (1:300, Abcam, ab6326) for 2 h, and then incubated with the secondary antibody Alexa Fluor 488 goat anti-rat IgG (H + L) (1:500, Invitrogen, A11006) for 2 h. Incubation with 300 nM DAPI for 15 min was used for counterstaining. Cells were examined using a Nikon microscope with Image-Pro Plus software for image analysis, and BrdU uptake was calculated in 10 microscopic fields.

2.4. MDC staining

Cells were grown on coverslips and treated with 5 μM BIX for 48 h. After treatment, monodansylcadaverine (MDC, Sigma) stock solution at 10 mM was diluted 200× in the culture medium and incubated for 30 min. Then the cells were washed with PBS, fixed in 4% PFA for 20 min, and examined using a Nikon microscope with Image-Pro Plus software for image analysis.

2.5. Immunofluorescence staining

Cells were grown on coverslips. After treated with 5 μM BIX, cells were washed with PBS, fixed in 4% PFA for 20 min, and permeabilized with 0.05% Triton X-100 for 15 min. Then the cells were blocked with 10% goat serum for 1 h, incubated with a primary antibody for overnight, and followed with the secondary antibody for 2 h. Incubation with 300 nM DAPI for 15 min was used for counterstaining. Cells were examined using a Nikon microscope with Image-Pro Plus software for image analysis. The primary antibodies rabbit anti-G9a (#3306, 1:200) and rabbit anti-LC3 (#4108S, 1:200) were purchased from Cell Signaling Tech. The primary antibody mouse anti-α-tubulin (AT819, 1:500) was purchased from Beyotime Biotech. The secondary antibodies Alexa Fluor 488 donkey anti-rabbit IgG (H + L) (1:2000, A21206) and Alexa Fluor 594 donkey anti-mouse IgG (H + L) (1:2000, A21203) were purchased from Invitrogen.

2.6. Apoptosis assay

Cells were plated in 10 cm plates and treated with 5 μM BIX for 48 h. Then cells were collected and resuspended in 100 μl binding buffer, incubated with 2.5 μl FITC Annexin-V and 5 μl PI (50 μg/ml) for 15 min, and analyzed by flow cytometry with CellQuest analysis software.

2.7. Tunel staining

Cells were grown on coverslips, treated with 5 μM BIX for 48 h and stained with Click-iT plus tunel assay kit (Invitrogen). Cells were washed with PBS, fixed in 4% paraformaldehyde (PFA) for 20 min, and permeabilized with 0.25% Triton X-100 for 15 min. The cells were incubated with TdT reaction buffer for 10 min, then TdT reaction mixture for 1 h, and then incubated with tunel reaction cocktail for 30 min. Incubation with 300 nM DAPI for 15 min was used for counterstaining. Cells were examined using a Nikon microscope with Image-Pro Plus software for image analysis.

2.8. Western blot assay

Cells were plated in 10 cm plates and treated with 5 μM BIX. After 48 h of treatment, cells were collected and proteins were extracted with RIPA lysis buffer and PMSF (Beyotime). Protein concentrations were determined with Enhanced BCA protein assay kit (Beyotime). Seventy micrograms of proteins were separated in 10% SDS-PAGE and transferred to PVDF membranes. After blocked with 5% nonfat milk for 2 h, the membrane was washed in TBST and incubated with primary antibody for overnight. Then the membrane was washed in TBST and incubated with horseradish peroxidase (HRP)-labeled secondary antibody for 2 h. The signal was visualized by the ECL reagent (Beyotime) and captured by western blotting detection instruments (Clinx Science). The primary antibodies rabbit anti-G9a (#3306, 1:1000) and rabbit anti-LC3 (#4108S, 1:1000) were purchased from Cell Signaling Tech. The primary antibody rabbit anti-H3K9me2 (ab32521, 1:500) was purchased from Abcam. The primary antibody rabbit anti-caspase 3 (sc-98785, 1:200) was purchased from Santa Cruz. The primary antibody mouse anti-α-tubulin (AT819, 1:1000) was purchased from Beyotime Biotech. The second antibodies including HRP-labeled goat anti-mouse IgG (H + L) (A0216.1:5000), and HRP-labeled goat anti-rabbit IgG (H + L) (A0208.1:5000) were purchased from Beyotime Biotech.

2.9. Soft agar colony formation assay

The cells were mixed with 0.3% soft agar (Sigma) and culture media, and seed in 6-well plates with a solidified bottom layer consisting of 0.6% soft agar and culture media at 1000 cell per well. After 20 days of treatment, the micrographs of cell colonies were taken by an inverted microscopy. Then the cells were stained with MTT and pictures were taken using a scanner (EPSON).

2.10. In vivo tumorigenic assay

Tca8113 cells were trypsinized and collected. 1×10^6 cells in 200 μl culture media were injected subcutaneously into the flanks of severe combined immune deficiency (SCID) mice. After 7 days of tumor growth, the mice were administered intraperitoneal injections of BIX (4 mg/kg) or sterile water once daily for 7 days. Tumor diameter were

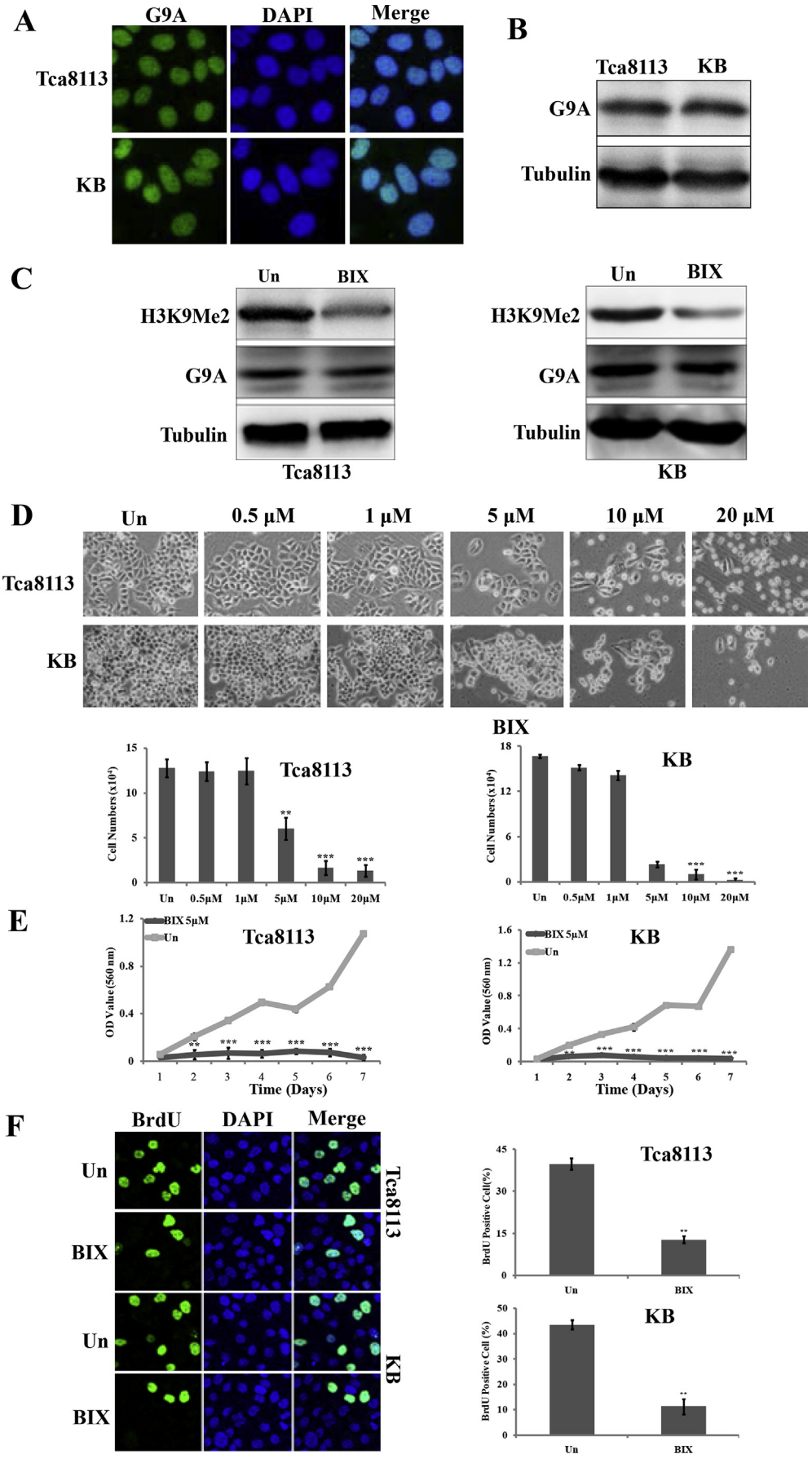
A
G9A
DAPI
Merge
Tca8113
KB
B
Tca8113
KB
G9A
Tubulin
C
Un
BIX
H3K9Me2
G9A
Tubulin
Tca8113
KB
D
Un
0.5 μM
1 μM
5 μM
10 μM
20 μM
Tca8113
KB
BIX
Cell Numbers (x10⁴)
Un
0.5μM
1μM
5μM
10μM
20μM
E
BIX 5μM
Un
OD Value (560 nm)
Time (Days)
F
BrdU
DAPI
Merge
Un
BIX
BrdU Positive Cell(%)

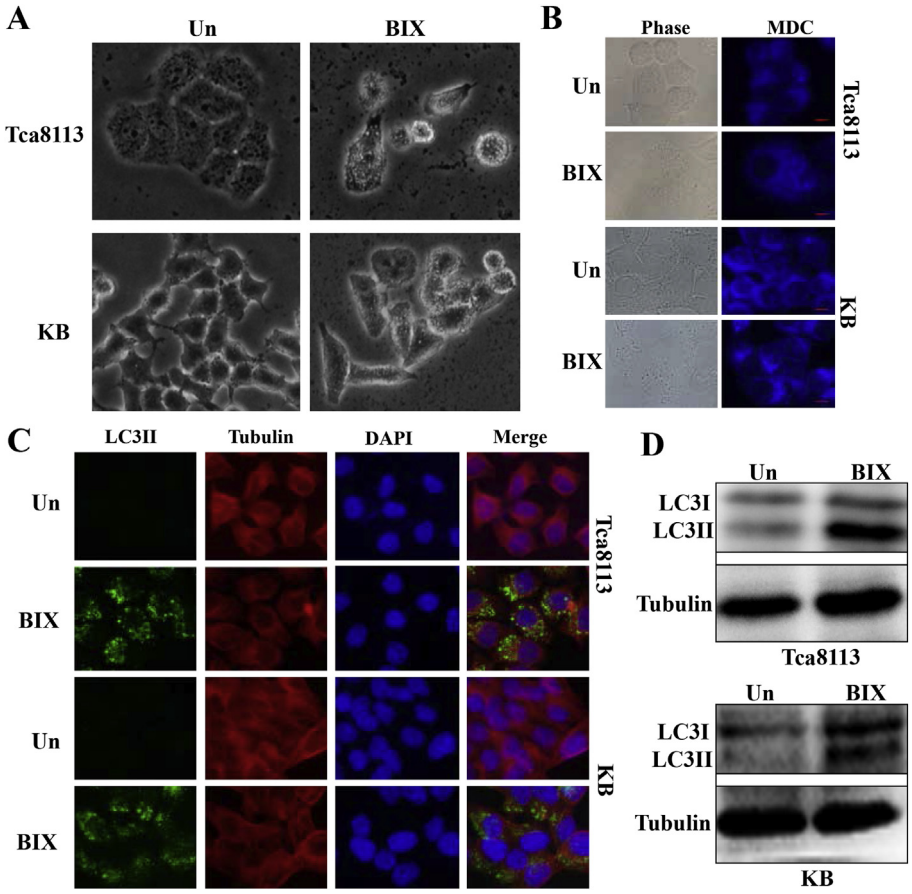

Fig. 2. Inhibition of G9a induced autophagy in OSCC cells. A. After being treated with 5 μM BIX for 48 h, membranous vacuoles were found in Tca8113 and KB cells. B. After being treated with 5 μM BIX for 48 h, autophagic vacuoles was examined by MDC staining. C. After being treated with 5 μM BIX for 48 h, autophagy-related protein LC3-II was examined by immunofluorescence staining. Cells were stained with an antibody against LC3-II (green) and tubulin (red), and counterstained with DAPI (blue). D. After being treated with 5 μM BIX for 48 h, the protein expression of LC3-II was examined by western blot assay. (For interpretation of the references to color in this figure legend, the reader is referred to the web version of this article.)

measured with digital calipers every day, and tumor volume was calculated (volume = length × width^2 × 0.5236). After treatment, the mice were sacrificed by CO_2, and tumors were measured and weighed. All animal experiments were pre-approved by the Institutional Animal Care and Use Committee of our university.

2.11. Statistical analysis

Each experiment was repeated at least three times. The results were presented as mean ± SD. The two-tailed Student's t-test was performed for paired samples. $p < 0.05$ was considered statistically significant.

3. Results

3.1. *G9a* is expressed in OSCC cells

Firstly to check G9a expression in OSCC cells, we performed immunofluorescence staining and western blot assay of G9a in Tca8113 and KB cells. The result showed that G9a is commonly expressed in both cells (Fig. 1A and B), which suggested that G9a might play an important role in OSCC.

3.2. Inhibition of *G9a* reduced cell growth and proliferation in OSCC cells

Next we examined the functional consequence of G9a high expression in OSCC cells. Tca8113 and KB cells were treated with BIX, a special inhibitor of G9a, at different concentration for 48 h. The result showed that BIX at concentration higher than 5 μM led to dramatically decrease in cell number compared with control (Fig. 1D). Then we confirmed that G9a activity is actually repressed after 5 μM BIX treatment through western blot assay of protein expression of H3K9me2, which was reported as a major product in G9a-mediated H3K9 methylation [13]. BIX treatment had no significant effect on G9a expression in OSCC cells at all, but led to a marked down-regulation of H3K9me2 (Fig. 1C). To further investigate the cytostatic effects of G9a inhibition, cell growth curve was

Fig. 1. Inhibition of G9a reduced cell growth and proliferation in OSCC cells. A. G9a expression was examined by immunofluorescence staining in Tca8113 and KB cells. Cells were stained with an antibody against G9a (green), and counterstained with DAPI (blue). B. G9a expression was examined by western blot assay. C. After being treated with 5 μM BIX for 48 h, the protein expression of G9a and H3K9me2 in Tca8113 and KB cells was investigated by western blot assay. D. Cell morphologic observation and cell counting after BIX treatment for 48 h. **$p < 0.01$. ***$p < 0.001$. E. After being treated with 5 μM BIX, cell growth was tested by MTT assay. **$p < 0.01$. ***$p < 0.001$. F. After being treated with 5 μM BIX for 48 h, cell proliferation was evaluated by Brdu immunofluorescence staining. Cells were stained with an antibody against Brdu (green), and counterstained with DAPI (blue). The percentage of Brdu positive cells was calculated from 10 randomly selected fields. **$p < 0.01$. (For interpretation of the references to color in this figure legend, the reader is referred to the web version of this article.)

determined by MTT assay. The result showed that 5 μM BIX dramatically inhibits cell growth in a time-dependent manner in both cells (Fig. 1E). In addition, Brdu staining was employed to detect the effect of G9a inhibition on DNA synthesis. After treated with 5 μM BIX for 48 h, the Brdu-positive cells significantly decreased in both cells compared with the control (Fig. 1F). All together, these results showed that G9a inhibition could reduce cells growth and proliferation in OSCC cells.

3.3. Inhibition of G9a induced autophagy in OSCC cells

After inhibition of G9a with BIX, we found the appearance of large membranous vacuoles in the cytoplasm in Tca8113 and KB cells, which is a characteristic feature of cells undergoing autophagy (Fig. 2A). So we performed MDC staining for autophagic vacuoles. BIX-treated cells exhibited higher fluorescent density and more MDC-labeled particles in Tca8113 and KB cells compared with

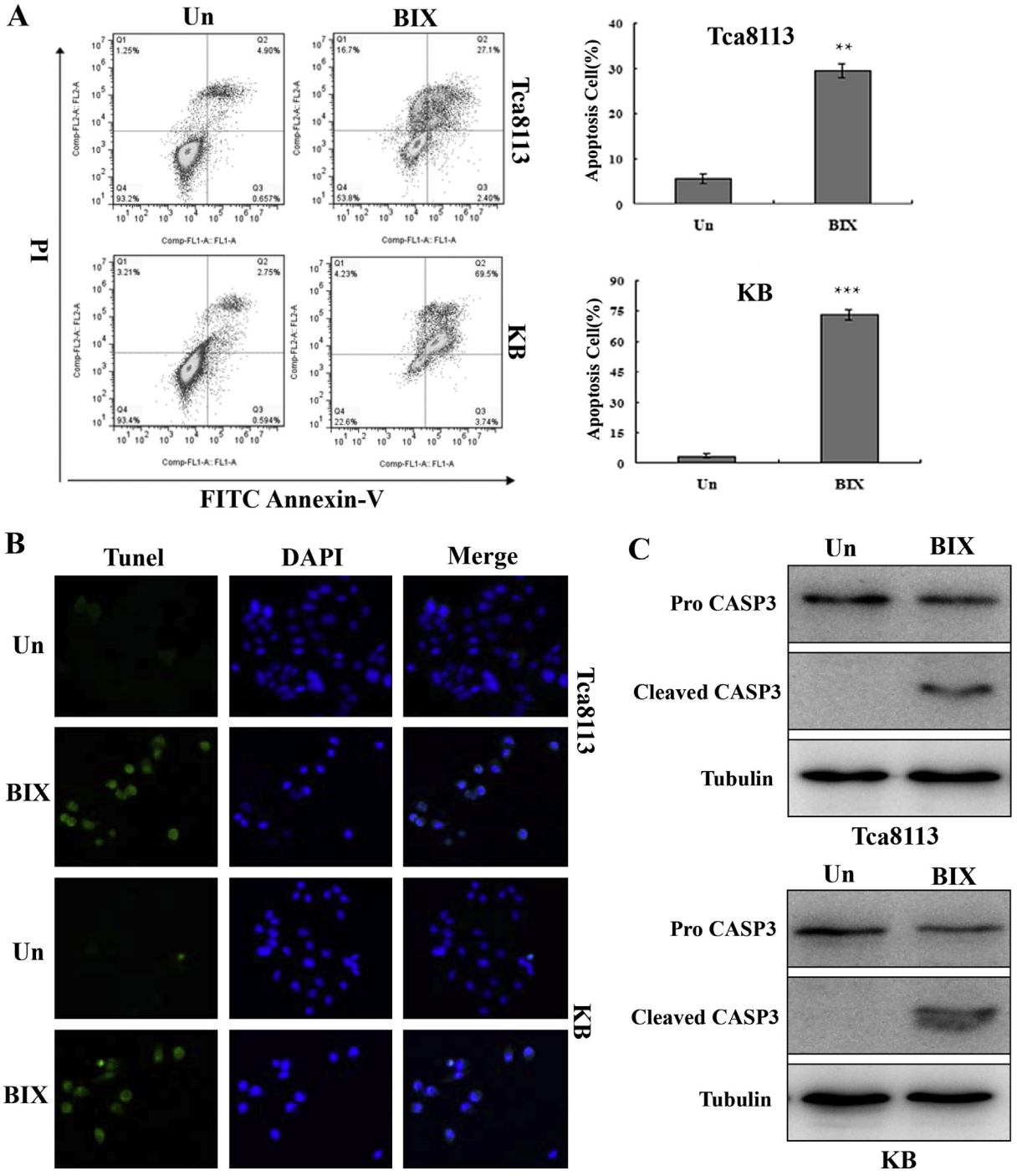

Fig. 3. Inhibition of G9a induced apoptosis in OSCC cells. A. After being treated with 5 μM BIX for 48 h, cell apoptosis of Tca8113 and KB cells was examined by FITC Annexin-V and PI labeling. **p < 0.01. ***p < 0.001. B. After being treated with 5 μM BIX for 48 h, cell apoptosis was examined by tunel staining. Cells were stained with tunnel assay kit (green), and counterstained with DAPI (blue). C. After being treated with 5 μM BIX for 48 h, the protein expression of caspase 3 was examined by western blot assay. CASP3, caspase 3. (For interpretation of the references to color in this figure legend, the reader is referred to the web version of this article.)

controls (Fig. 2B). To further confirm that inhibition of G9a induces autophagy in Tca8113 and KB cells, the expression of microtubule-associated protein 1 light chain 3 (LC3) was examined. LC3 is the first known mammalian protein that is specifically associated with the autophagosomal membrane that exists as two forms, the 18 kDa cytosolic LC3-I and 16 kDa autophagosome membrane-bound LC3-II. Under normal conditions, LC3-I is distributed uniformly throughout the nucleus and cytoplasm. In autophagic cells, LC3-I is processed into the lower molecular form LC-II and translocates into autophagosome membranes, appearing as bright puncta [17]. As shown in Fig. 2C, the number and intensity of punctate LC3 fluorescence increased after BIX treatment. The same result was found in western blot assay of LC3. BIX treatment significant increased the expression of LC3-II (Fig. 2D). These results suggested that inhibition of G9a could induce autophagy in OSCC cells.

3.4. Inhibition of G9a induced apoptosis in OSCC cells

Previous studies have demonstrated that coregulation of apoptosis and autophagy can participate in mammalian cell death [18]. In order to determine whether inhibition of G9a induced apoptosis in Tca8113 and KB cells, we performed a flow cytometry assay by FITC Annexin-V and PI staining. The results demonstrated that 5 μM BIX obviously increased apoptotic cells proportion after 48 h treatment (Fig. 3A). The apoptosis cell proportion increased from 5.56% to 29.5% in Tca8113 cells and from 3.34% to 73.24% in KB cells. The cell apoptosis was further confirmed by tunel staining.

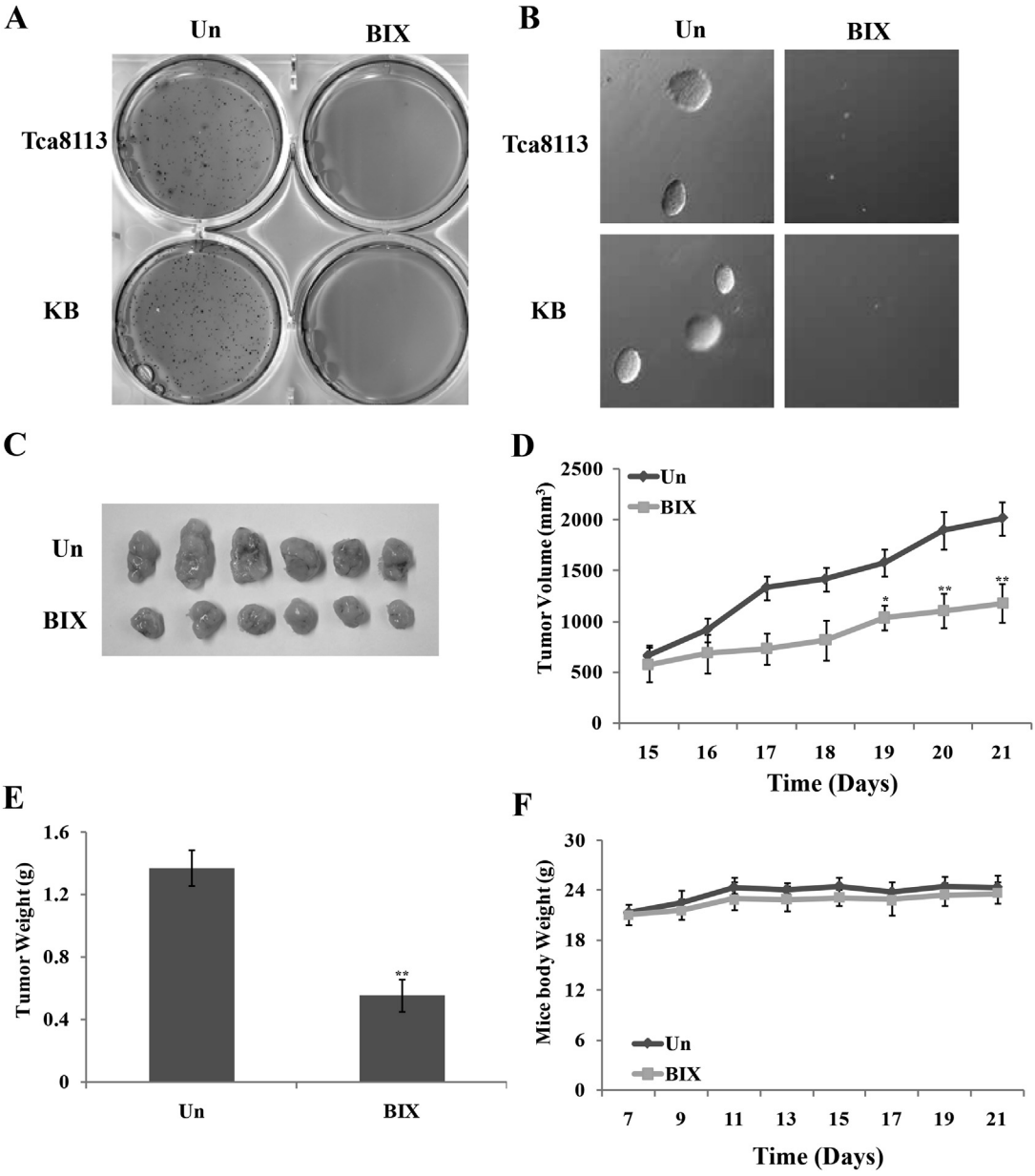

Fig. 4. Inhibition of G9a reduced colony formation in soft agar and repressed tumor growth in mouse xenograph model. A. After being treated with 5 μM BIX for 20d in soft agar, the cell colonies of Tca8113 and KB cells were stained with MTT and pictures were taken with a scanner. B. After being treated with 5 μM BIX for 20d in soft agar, the micrographs of cell colonies were taken by an inverted microscopy. C. The photo of SCID mice xenograft tumor after being treated with BIX. D. The xenograft tumor volume after being treated with BIX. *p < 0.05. **p < 0.01. E. The xenograft tumor weight after being treated with BIX. **p < 0.01. F. The SCID mice body weight after being treated with BIX.

After 48 h treatment of BIX, the tunnel-positive cells significantly increased in both cells compared with the control (Fig. 3B). We also examined the activation of caspase 3. After 48 h treatment of BIX, the 17KD cleaved fragment of caspase 3 was clearly detected (Fig. 3C). Taken together, these results showed that inhibition of G9a also induced apoptosis in OSCC cells.

3.5. Inhibition of G9a reduced colony formation in soft agar and repressed tumor growth in mouse xenograph model

To determine the effect of G9a inhibition on anchorage-independent growth of Tca8113 and KB cells, we performed a soft agar colony formation assay. After 20 days of treatment, 5 μM BIX obviously inhibited the colony formation. The size and number of colonies were dramatically decreased (Fig. 4A and B). These results suggested that inhibition of G9a could inhibit colony formation capacity in OSCC cells. We further examined the effect of inhibition of G9a on tumor growth in mouse xenograph model. Tca8113 cells were injected into SCID mice subcutaneously. After 7 days of tumor growth, BIX was used for 7 days. The result showed that BIX treatment inhibited tumor growth dramatically (Fig. 4C–E). In addition, the injection of BIX did not affect the animal weight (Fig. 4F) and behavior. These results suggested that inhibition of G9a could inhibit OSCC growth in vivo.

4. Discussion

Overexpression of G9a has been observed in many types of human cancers and is associated with poor prognosis [15,19,20]. Inhibition of G9a has been reported to reduce cell growth and induce senescence in a variety of cancer types [21–23]. In this study, we found that G9a was expressed in two OSCC cell lines (Tca8113 and KB) and inhibition of G9a using a specific inhibitor BIX obviously reduced the expression of H3K9me2, a major product in G9a-mediated H3K9 methylation. So we investigated the effect of G9a inhibition on OSCC growth in vitro and in vivo. The results showed that G9a was important to cell proliferation, clonogenesis and tumorigenicity. Inhibition of G9a significantly reduced cell growth, colony formation and xenograph tumor growth. These finding suggested that G9a might have oncogenic activity in OSCC and change of epigenetic patterns regulated by G9a would be helpful for OSCC treatment.

Autophagy is an evolutionarily conserved cellular catabolic process that maintains cellular homeostasis with degrading and recycling intracellular macromolecules and organelles in response to cell stress [24,25]. Autophagy can be induced in several circumstances including hypoxia, aging, nutrient deprivation, as well as chemical and radiation cancer therapy [26,27]. As an adaptive response to cell stress, autophagy usually plays an important role in removing damaged organelles and recycling of nutrients and energy [28]. On the contrary, excessive autophagy causing over-consumption of critical cellular components is responsible for autophagic cell death or type II programmed cell death which is resembled to apoptosis [28,29]. It was reported that inhibition of G9a could induce autophagy in breast and colorectal cancers [22], pancreatic cancer [30], neuroblastoma [23,31], cervix cancer and osteosarcoma [23]. In this study, we found that inhibition of G9a induced cell autophagy in OSCC which was characterized by MDC stainings of vesicle formation and the conversion of LC3-I to LC3-II. Therefore, we speculated that autophagy might be one of the mechanisms by which G9a epigenetically controlled cell growth in OSCC.

Inhibition of G9a was also reported to promote apoptosis in breast cancer [32], bladder and lung cancers [14]. In this study, we also found that inhibition of G9a induced cell apoptosis in OSCC which was confirmed by Annexin-v staining, tunnel staining and the expression of cleaved caspase 3. Thus apoptosis might be another mechanism by which G9a epigenetically controlled cell growth in OSCC. Taken together, our result suggested that G9a might control OSCC cell growth via multiple routes. Recently, it was reported that inhibition of G9a induces autophagy not apoptosis in two head and neck squamous carcinoma cell (HNSCC) lines (SAS and FaDu) [33], which was different from our findings. Therefore, it was particularly interesting to identify the molecular mechanism of the regulation mediated by G9a in OSCC growth.

In summary, our result demonstrated that inhibition of G9a could reduce growth and proliferation, and induce autophagy and apoptosis in OSCC. It indicated that G9a might be a potential epigenetic target for OSCC treatment.

Conflict of interest

The authors declare no potential conflicts of interest.

Acknowledgments

This study was supported by Nature Science Foundation of Chongqing (cstc2011jjA10086) and program for innovation team building at institutions of higher education in Chongqing in 2013.

Transparency document

Transparency document related to this article can be found online at http://dx.doi.org/10.1016/j.bbrc.2015.01.068.

References

[1] F. Bray, R. Sankila, J. Ferlay, et al., Estimates of cancer incidence and mortality in Europe in 1995, Eur. J. Cancer 38 (1) (2002) 99–166.
[2] S.H. Landis, T. Murray, S. Bolden, et al., Cancer statistics, 1999, CA Cancer J. Clin. 49 (1) (1999) 8–31, 1.
[3] D.M. Parkin, F. Bray, J. Ferlay, et al., Global cancer statistics, 2002, CA Cancer J. Clin. 55 (2) (2005) 74–108.
[4] R. Siegel, D. Naishadham, A. Jemal, Cancer statistics for Hispanics/Latinos, 2012, CA Cancer J. Clin. 62 (5) (2012) 283–298.
[5] Y.S. Cheng, T. Rees, J. Wright, A review of research on salivary biomarkers for oral cancer detection, Clin. Transl. Med. 3 (1) (2014) 3.
[6] O. Bettendorf, J. Piffko, A. Bankfalvi, Prognostic and predictive factors in oral squamous cell cancer: important tools for planning individual therapy? Oral Oncol. 40 (2) (2004) 110–119.
[7] G. Egger, G. Liang, A. Aparicio, et al., Epigenetics in human disease and prospects for epigenetic therapy, Nature 429 (6990) (2004) 457–463.
[8] K.E. Bachman, B.H. Park, I. Rhee, et al., Histone modifications and silencing prior to DNA methylation of a tumor suppressor gene, Cancer Cell. 3 (1) (2003) 89–95.
[9] D.Q. Calcagno, C.O. Gigek, E.S. Chen, et al., DNA and histone methylation in gastric carcinogenesis, World J. Gastroenterol. 19 (8) (2013) 1182–1192.
[10] M. Tachibana, K. Sugimoto, M. Nozaki, et al., G9a histone methyltransferase plays a dominant role in euchromatic histone H3 lysine 9 methylation and is essential for early embryogenesis, Genes. Dev. 16 (14) (2002) 1779–1791.
[11] A.H. Peters, S. Kubicek, K. Mechtler, et al., Partitioning and plasticity of repressive histone methylation states in mammalian chromatin, Mol. Cell. 12 (6) (2003) 1577–1589.
[12] J.C. Rice, S.D. Briggs, B. Ueberheide, et al., Histone methyltransferases direct different degrees of methylation to define distinct chromatin domains, Mol. Cell. 12 (6) (2003) 1591–1598.
[13] Y. Shinkai, M. Tachibana, H3K9 methyltransferase G9a and the related molecule GLP, Genes. Dev. 25 (8) (2011) 781–788.
[14] H.S. Cho, J.D. Kelly, S. Hayami, et al., Enhanced expression of EHMT2 is involved in the proliferation of cancer cells through negative regulation of SIAH1, Neoplasia 13 (8) (2011) 676–684.
[15] K.T. Hua, M.Y. Wang, M.W. Chen, et al., The H3K9 methyltransferase G9a is a marker of aggressive ovarian cancer that promotes peritoneal metastasis, Mol. Cancer 13 (2014) 189.
[16] M.W. Chen, K.T. Hua, H.J. Kao, et al., H3K9 histone methyltransferase G9a promotes lung cancer invasion and metastasis by silencing the cell adhesion molecule Ep-CAM, Cancer Res. 70 (20) (2010) 7830–7840.
[17] W.T. Liu, C.H. Lin, M. Hsiao, et al., Minocycline inhibits the growth of glioma by inducing autophagy, Autophagy 7 (2) (2011) 166–175.

[18] T. Tomic, T. Botton, M. Cerezo, et al., Metformin inhibits melanoma development through autophagy and apoptosis mechanisms, Cell. Death Dis. 2 (2011) e199.
[19] J.H. Chen, K.T. Yeh, Y.M. Yang, et al., High expressions of histone methylation- and phosphorylation-related proteins are associated with prognosis of oral squamous cell carcinoma in male population of Taiwan, Med. Oncol. 30 (2) (2013) 513.
[20] X. Zhong, X. Chen, X. Guan, et al., Overexpression of G9a and MCM7 in oesophageal squamous cell carcinoma is associated with poor prognosis, Histopathology 66 (2) (2015) 192–200.
[21] Y. Yuan, Q. Wang, J. Paulk, et al., A small-molecule probe of the histone methyltransferase G9a induces cellular senescence in pancreatic adenocarcinoma, ACS Chem. Biol. 7 (7) (2012) 1152–1157.
[22] Y. Kim, Y.S. Kim, D.E. Kim, et al., BIX-01294 induces autophagy-associated cell death via EHMT2/G9a dysfunction and intracellular reactive oxygen species production, Autophagy 9 (12) (2013) 2126–2139.
[23] J. Ding, T. Li, X. Wang, et al., The histone H3 methyltransferase G9A epigenetically activates the serine-glycine synthesis pathway to sustain cancer cell survival and proliferation, Cell. Metab. 18 (6) (2013) 896–907.
[24] D. Glick, S. Barth, K.F. Macleod, Autophagy: cellular and molecular mechanisms, J. Pathol. 221 (1) (2010) 3–12.
[25] N. Mizushima, B. Levine, A.M. Cuervo, et al., Autophagy fights disease through cellular self-digestion, Nature 451 (7182) (2008) 1069–1075.
[26] T. Kanzawa, Y. Kondo, H. Ito, et al., Induction of autophagic cell death in malignant glioma cells by arsenic trioxide, Cancer Res. 63 (9) (2003) 2103–2108.
[27] S. Paglin, T. Hollister, T. Delohery, et al., A novel response of cancer cells to radiation involves autophagy and formation of acidic vesicles, Cancer Res. 61 (2) (2001) 439–444.
[28] M.C. Maiuri, E. Zalckvar, A. Kimchi, et al., Self-eating and self-killing: crosstalk between autophagy and apoptosis, Nat. Rev. Mol. Cell. Biol. 8 (9) (2007) 741–752.
[29] P.G. Clarke, J. Puyal, Autophagic cell death exists, Autophagy 8 (6) (2012) 867–869.
[30] Y. Yuan, A.J. Tang, A.B. Castoreno, et al., Gossypol and an HMT G9a inhibitor act in synergy to induce cell death in pancreatic cancer cells, Cell. Death Dis. 4 (2013) e690.
[31] X.X. Ke, D. Zhang, S. Zhu, et al., Inhibition of H3K9 methyltransferase G9a repressed cell proliferation and induced autophagy in neuroblastoma cells, PLoS One 9 (9) (2014) e106962.
[32] J. Huang, J. Dorsey, S. Chuikov, et al., G9a and Glp methylate lysine 373 in the tumor suppressor p53, J. Biol. Chem. 285 (13) (2010) 9636–9641.
[33] K.C. Li, K.T. Hua, Y.S. Lin, et al., Inhibition of G9a induces DUSP4-dependent autophagic cell death in head and neck squamous cell carcinoma, Mol. Cancer 13 (2014) 172.